Acta Mech 233, 4047–4062 (2022)
https://doi.org/10.1007/s00707-022-03303-6

ORIGINAL PAPER

Dmitry K. Demskoi · Colin Rogers · Wolfgang K. Schief

On 2+1-dimensional fibre-reinforced fluid motions: a magnetohydrodynamics nexus

Received: 28 May 2022 / Accepted: 4 July 2022 / Published online: 1 September 2022

Abstract An intrinsic geometric decomposition is applied to provide via a canonical third-order nonlinear equation a connection between 2+1-dimensional fibre-reinforced motions of a fluid and a magnetohydrodynamic system. A Lagrange-type parametrisation is introduced, whereby both geometric and algebraic properties of certain non-steady magnetohydrodynamic motions may be established.

1 Introduction

In [1], a novel intrinsic geometric formulation was introduced in the context of the kinematic analysis of certain hydrodynamic motions. The representations contained therein have subsequently proved to have diverse applications in both nonlinear continuum mechanics and soliton theory. In magnetohydrodynamics, application has been made to isolate conducting motions in which the Maxwellian surfaces contain the streamlines as geodesics and the magnetic lines as parallels [2]. In soliton theory, the anholonomic representations of [1] have been adopted in [3] to derive, in a purely geometric manner, both the auto-Bäcklund transformation and a Lax pair for the nonlinear Schrödinger (NLS) equation. NLS soliton surfaces of both 'smoke ring' and spatial breather-type may be thereby constructed [4]. A connection between a previously well-studied class of spatial hydrodynamic motions and the integrable solitonic Heisenberg spin equation subject to a natural geometric constraint was uncovered in [5] by means of an intrinsic geometric representation. This novel link was subsequently elaborated upon in [6]. Later a connection was thereby made in [7] between this Heisenberg spin reduction and a classical problem in hydrodynamics posed by Gilbarg [8]. In recent work, such Heisenberg spin connection has been extended to spatial relativistic gasdynamics [9]. Motions subject to a complex-lamellar geometric constraint have been investigated via intrinsic anholonomic representations in both spatial gasdynamics [10] and magnetohydrodynamics [11]. In magnetohydrostatics [12], an integrable Heisenberg spin reduction obtains *mutatis mutandis* to that originally derived in hydrodynamics and was applied to determine geometric configurations in which the constant total magnetic pressure surfaces comprise nested tori foliated in accordance with the admitted constraint.

Dmitry K. Demskoi, Colin Rogers and Wolfgang K. Schief have contributed equally to this work.

D. K. Demskoi
School of Computing, Mathematics and Engineering, Charles Sturt University, Wagga Wagga, NSW 2678, Australia
E-mail: ddemskoy@csu.edu.au

C. Rogers · W. K. Schief (✉)
School of Mathematics and Statistics, The University of New South Wales, Sydney, NSW 2052, Australia
E-mail: w.schief@unsw.edu.au

C. Rogers
E-mail: c.rogers@unsw.edu.au

The connection in geometric terms between privileged motions of inextensible curves and modern soliton theory may be said to have its origin in the analysis by Da Rios [13] of the spatial motion of an isolated vortex filament embedded in an unbounded viscous liquid. Therein, what has come to be termed the localised induction approximation was invoked to derive a pair of coupled evolution equations for the curvature and torsion of the filament. These results were later to be incorporated in a survey by Levi-Civita [14]. Hasimoto [15], motivated by a geometric study in [16], was to establish that the classical Da Rios system is equivalent, without approximation, to the canonical nonlinear Schrödinger equation of modern soliton theory. Indeed, the latter NLS equation may be generated in a purely geometric manner via privileged binormal motions of an inextensible curve [5].

A kinematic study of the motion of fibre-reinforced fluids has its origin in the work of Spencer [17]. The model therein comprised an incompressible fluid with embedded inextensible fibre lines convected by the motions. That the motion of inextensible curves appears in both the context of the motion of fibre-reinforced fluids and soliton theory indicated the potential existence of integrable structure of solitonic type admitted by the kinematic system of [17]. This indeed has proved to be the case. Thus, in [18] a class of deformations inherent in the kinematic system of Spencer [17] has been linked to the AKNS inverse scattering scheme via the integrable modified Korteweg-de-Vries (mkdV) solitonic hierarchy.

In [19,20], the geometric formalism previously adopted in hydrodynamics, magnetohydrostatics, magnetohydrodynamics, and soliton theory was used to investigate the kinematic conditions attendant upon the motion of a fibre-reinforced fluid. Kinematically admissible spatial motions were thereby obtained in which the fibres are geodesic windings on nested toroidal surfaces. In the case of purely planar motion, it was shown that the kinematic relations may be encapsulated in a novel third-order nonlinear equation. Remarkably, this admits a particular reduction to a solitonic system which is related to the classical sine-Gordon equation as originally obtained in the context of pseudospherical surfaces by Bour [21]. The kinematic conditions in this reduction admit both a Bäcklund transformation [22] and a duality property. In [23], the reduction of the kinematic system of [17] to a third-order nonlinear equation has been extended to 2+1-dimensional motions and underlying integrable solitonic structure again isolated. The geometry and integrability of steady motions of an ideal fibre-reinforced fluid in a curved stratum have been the subject of [24].

In [25], it has recently been established that the canonical third-order nonlinear equation derived via intrinsic geometric representations in [19,20] may likewise be shown to arise in steady two-dimensional magnetohydrodynamics subject to analogous kinematic conditions. This connection was used to isolate novel classes of time-independent conducting motions. Here, this nexus between the theory of the motion of fibre-reinforced liquids and magnetohydrodynamics is extended to 2+1-dimensional motions. In that connection, a geometric Lagrangian-type parameterisation is introduced. Geometric and algebraic properties of the time-dependent magnetohydrodynamic motions are described in detail. In overall terms, the preceding attests to the utility of the imposition of natural geometric constraints to isolate a hidden integrable structure in nonlinear continuum mechanics [26].

2 Planar fibre-reinforced fluid motions

The ideal fibre-reinforced fluid model considered here consists of an incompressible liquid which is inextensible along 'fibre' lines which occupy the volume of the fluid by which they are convected [17]. Thus, if a generic fibre direction is characterised by a unit vector $\boldsymbol{t}$ and $\boldsymbol{q}$ denotes the fluid velocity, then the kinematic condition which encodes both the convection requirement and inextensibility of the fibres is given by

$$(\partial_t + \boldsymbol{q} \cdot \nabla)\, \boldsymbol{t} = (\boldsymbol{t} \cdot \nabla)\boldsymbol{q}. \tag{1}$$

This evolution equation is augmented by the continuity equation

$$\operatorname{div} \boldsymbol{q} = 0 \tag{2}$$

which follows from the incompressibility of the fluid.

2.1 Geometric decomposition and reformulation

The equation of motion (1) may be regarded as the compatibility condition which guarantees the existence of a function ρ obeying the pair of equations

$$\boldsymbol{t} \cdot \nabla \rho = 1, \quad (\partial_t + \boldsymbol{q} \cdot \nabla)\rho = 0. \tag{3}$$

Geometrically, this means that ρ constitutes the arc length along the fibres which is convected by the fluid flow. It is observed that this is consistent with the assumption that the fibres are inextensible. It is therefore convenient to introduce the directional derivatives

$$D_s = \boldsymbol{t} \cdot \nabla, \quad D_n = \boldsymbol{n} \cdot \nabla, \tag{4}$$

where $\boldsymbol{n}$ denotes the principal (unit) normal to the fibres. If κ is the curvature of the fibres, then the orthonormal pair $(\boldsymbol{t}, \boldsymbol{n})$ obeys the Serret-Frenet equations [27]

$$D_s \begin{pmatrix} \boldsymbol{t} \\ \boldsymbol{n} \end{pmatrix} = \begin{pmatrix} 0 & \kappa \\ -\kappa & 0 \end{pmatrix} \begin{pmatrix} \boldsymbol{t} \\ \boldsymbol{n} \end{pmatrix} \tag{5}$$

and, analogously,

$$D_n \begin{pmatrix} \boldsymbol{t} \\ \boldsymbol{n} \end{pmatrix} = \begin{pmatrix} 0 & \theta \\ -\theta & 0 \end{pmatrix} \begin{pmatrix} \boldsymbol{t} \\ \boldsymbol{n} \end{pmatrix} \tag{6}$$

with $\theta = \operatorname{div} \boldsymbol{t}$ being the negative of the curvature of the trajectories which are orthogonal to the fibres. Furthermore, $\boldsymbol{t}$ and $\boldsymbol{n}$ may be parametrised by an angle φ according to

$$\boldsymbol{t} = \begin{pmatrix} \cos\varphi \\ \sin\varphi \end{pmatrix}, \quad \boldsymbol{n} = \begin{pmatrix} -\sin\varphi \\ \cos\varphi \end{pmatrix}. \tag{7}$$

The existence of the fibre lines gives rise to a natural time-dependent orthogonal coordinate system $(x(s, n, \tau), y(s, n, \tau))$ on the plane, where $\tau = t$ and the fibres and orthogonal trajectories are parametrised by s and n, respectively.

Remarkably, it has been shown [23] that, in terms of the independent variables s, n, and τ, the kinematic equations (1) and (2) may be reformulated as a third-order partial differential equation in which time only enters parametrically. This is the content of the following theorem.

Theorem 1 *Given a solution $(\rho, \psi(\rho, n))$ of the partial differential equation*

$$\left(\frac{\rho_{sn}}{\psi}\right)_n + \psi_{\rho\rho}\rho_s = 0, \tag{8}$$

wherein ρ may depend parametrically on τ and a solution of the governing equations (1), (2) is given by

$$\boldsymbol{q} = v\boldsymbol{t} + w\boldsymbol{n}, \tag{9}$$

where the angle φ parametrising $\boldsymbol{t}$ and $\boldsymbol{n}$ is determined by the compatible system

$$\varphi_s = -\frac{\rho_{ns}}{\psi}, \quad \varphi_n = \psi_\rho, \tag{10}$$

and the velocity components v and w read

$$v = x_\tau \cos\varphi + y_\tau \sin\varphi - \rho_\tau, \quad w = -x_\tau \sin\varphi + y_\tau \cos\varphi \tag{11}$$

with the parametrisation of the Eulerian coordinates being obtained via integration of the compatible system

$$x_s = \rho_s \cos\varphi, \quad x_n = -\psi \sin\varphi, \quad y_s = \rho_s \sin\varphi, \quad y_n = \psi \cos\varphi \tag{12}$$

and $t = \tau$. At any instant t, the one-parameter family of fibres labelled by n is parametrised by s according to $(x, y)(s, n, \tau = t)$.

It is observed that the relations (12) imply that the metric of the plane and the gradient are given by

$$dx^2 + dy^2 = \rho_s^2 ds^2 + \psi^2 dn^2 \tag{13}$$

and

$$\nabla = \boldsymbol{t} D_s + \boldsymbol{n} D_n = \frac{\boldsymbol{t}}{\rho_s}\partial_s + \frac{\boldsymbol{n}}{\psi}\partial_n. \tag{14}$$

Hence, insertion of the parametrisation (7) into the Serret-Frenet-type equations (5) and (6) reveals, on use of (10), that

$$\kappa = -\frac{\rho_{sn}}{\rho_s \psi}, \quad \theta = \frac{\psi_\rho}{\psi}. \tag{15.1,2}$$

2.2 Lagrangian coordinates

It is readily shown [23] that the convective derivative adopts the compact form

$$\partial_t + \boldsymbol{q}\cdot\nabla = \partial_\tau - \frac{\rho_\tau}{\rho_s}\partial_s \tag{16}$$

in terms of the adapted coordinates s, n, and τ. If one applies the latter to the Eulerian coordinate vector $\boldsymbol{r}$, then one obtains

$$\boldsymbol{q} = (\partial_t + \boldsymbol{q}\cdot\nabla)\boldsymbol{r} = \boldsymbol{r}_\tau - \frac{\rho_\tau}{\rho_s}\boldsymbol{r}_s, \quad \boldsymbol{r} = \begin{pmatrix} x \\ y \end{pmatrix}, \tag{17}$$

which is seen to be consistent with the components (11) of the velocity $\boldsymbol{q}$. This observation suggests introducing the independent variables

$$(\mathsf{s}, \mathsf{n}, \mathsf{t}) = (\rho(s, n, \tau), n, \tau), \tag{18}$$

leading to

$$\partial_s = \rho_s\partial_\mathsf{s}, \quad \partial_n = \partial_\mathsf{n} + \rho_n\partial_\mathsf{s}, \quad \partial_\tau = \partial_\mathsf{t} + \rho_\tau\partial_\mathsf{s} \tag{19}$$

or, equivalently,

$$\partial_\mathsf{s} = \frac{1}{\rho_s}\partial_s = D_s, \quad \partial_\mathsf{n} = \partial_n - \frac{\rho_n}{\rho_s}\partial_s, \quad \partial_\mathsf{t} = \partial_\tau - \frac{\rho_\tau}{\rho_s}\partial_s = \partial_t + \boldsymbol{q}\cdot\nabla. \tag{20}$$

In particular, the equation of motion (1) is then simply represented by the commutativity

$$[\partial_t + \boldsymbol{q}\cdot\nabla, D_s] = [\partial_\mathsf{t}, \partial_\mathsf{s}] = 0, \tag{21}$$

and the particle lines of the fluid are given by $\boldsymbol{r}(\mathsf{s} = \text{const}, \mathsf{n} = \text{const}, \mathsf{t})$ since

$$\boldsymbol{q} = \boldsymbol{r}_\mathsf{t}. \tag{22}$$

In summary, the above confirms that not only does $\rho = \mathsf{s}$ represent the arc length along the fibres which are convected by the fluid, it also labels the particles on the fibres $\mathsf{n} = \text{const}$ as they deform as a function of time. Thus, the independent variables s and n constitute material (Lagrangian) coordinates.

The above change of independent variables is naturally accompanied by the introduction of a new dependent variable given by

$$\rho_n =: R(\mathsf{s}, \mathsf{n}, \mathsf{t}). \tag{23}$$

The pair of equations (10) determining φ then adopts the form

$$\varphi_\mathsf{s} = -\frac{R_\mathsf{s}}{\psi}, \quad \varphi_\mathsf{n} = \psi_\mathsf{s} + \frac{RR_\mathsf{s}}{\psi}, \quad \psi = \psi(\mathsf{s}, \mathsf{n}) \tag{24}$$

so that the associated compatibility condition $(\varphi_\mathsf{s})_\mathsf{n} = (\varphi_\mathsf{n})_\mathsf{s}$ produces the second-order equation

$$\left(\frac{R_\mathsf{s}}{\psi}\right)_\mathsf{n} + \left(\frac{RR_\mathsf{s}}{\psi}\right)_\mathsf{s} + \psi_{\mathsf{ss}} = 0 \tag{25}$$

which constitutes the third-order equation (8) formulated in terms of the new (in)dependent variables. Once R is known, the function ρ is obtained by solving the first-order ordinary differential equation

$$\rho_n = R(\rho(s, n, \tau), n, \tau). \tag{26}$$

3 The magnetohydrodynamic equations

Here, the concern is with the 2+1-dimensional reduction of the non-dissipative magnetohydrodynamic system

$$\operatorname{div} \boldsymbol{q} = 0, \tag{27.1}$$
$$\boldsymbol{q}_t + (\boldsymbol{q} \cdot \nabla)\boldsymbol{q} - \operatorname{curl} \boldsymbol{H} \times \boldsymbol{H} + \nabla p = \boldsymbol{0}, \tag{27.2}$$
$$\operatorname{div} \boldsymbol{H} = 0, \tag{27.3}$$
$$\boldsymbol{H}_t = \operatorname{curl}(\boldsymbol{q} \times \boldsymbol{H}), \tag{27.4}$$

where $\boldsymbol{H}$ and p denote, in turn, the magnetic field and pressure. The density and magnetic permeability are assumed to be constant and have been scaled to unity. The solution of the magnetic induction and Faraday equations (27.3, 27.4) is readily seen to be

$$\boldsymbol{H} = \nabla A \times \boldsymbol{b}, \tag{28}$$

where the magnetic flux A is convected by the fluid, that is,

$$(\partial_t + \boldsymbol{q} \cdot \nabla)A = 0. \tag{29}$$

The (constant) unit vector $\boldsymbol{b}$ is orthogonal to the plane in which the motion takes place. If we reformulate the momentum equation (27.2) as

$$\boldsymbol{q}_t + \operatorname{curl} \boldsymbol{q} \times \boldsymbol{q} - \operatorname{curl} \boldsymbol{H} \times \boldsymbol{H} + \nabla \left(p + \frac{\boldsymbol{q}^2}{2} \right) = \boldsymbol{0}, \tag{30}$$

then its compatibility condition

$$\operatorname{curl}[\boldsymbol{q}_t + \operatorname{curl} \boldsymbol{q} \times \boldsymbol{q} - \operatorname{curl} \boldsymbol{H} \times \boldsymbol{H}] = \boldsymbol{0} \tag{31}$$

guaranteeing the existence of the pressure p may be formulated as [25]

$$(\partial_t + \boldsymbol{q} \cdot \nabla)\omega^q = \boldsymbol{H} \cdot \nabla \omega^H, \quad \omega^q = \boldsymbol{b} \cdot \operatorname{curl} \boldsymbol{q}, \quad \omega^H = \boldsymbol{b} \cdot \operatorname{curl} \boldsymbol{H} \tag{32}$$

with ω^q and ω^H being the vorticity and current density, respectively.

In [25], it has been demonstrated in the steady case that it is natural to assume that there exist notional inextensible 'fibres' embedded in the fluid which are convected by the fluid flow. It turns out that this is also the case in the current setting so that we now require $\boldsymbol{q}$ to obey the kinematic equations (1) and (2) for a unit vector field $\boldsymbol{t}$ to be determined. An immediate consequence of this assumption is that the magnetic flux A is a function of ρ and n since both quantities are convected by the fluid. Here, for simplicity, we confine ourselves to the case of A being a function of ρ only, that is,

$$A = A(\rho). \tag{33}$$

On use of the decomposition (14), we conclude that

$$\boldsymbol{H} = B \left(\frac{\rho_n}{\psi} \boldsymbol{t} - \boldsymbol{n} \right), \quad B = A'(\rho) \tag{34}$$

so that

$$\boldsymbol{H} \cdot \nabla = \frac{B}{\psi} \left(\frac{\rho_n}{\rho_s} \partial_s - \partial_n \right). \tag{35}$$

The compatibility condition (32) may therefore be written as

$$(\rho_s \partial_\tau - \rho_\tau \partial_s)(\psi \omega^q) + (\rho_s \partial_n - \rho_n \partial_s)(B \omega^H) = 0. \tag{36}$$

In order to find explicit expressions for the vorticity ω^q and the current density ω^H, we note that the curl of any vector field $\boldsymbol{F} = F^{(t)}\boldsymbol{t} + F^{(n)}\boldsymbol{n}$ reads

$$\boldsymbol{b} \cdot \operatorname{curl} \boldsymbol{F} = \boldsymbol{b} \cdot (\nabla \times \boldsymbol{F}) = -D_n F^{(t)} + D_s F^{(n)} + \kappa F^{(t)} + \theta F^{(n)} \tag{37}$$

by virtue of the Serret-Frenet-type relations (5) and (6). Here, we have made the choice $\boldsymbol{b} := \boldsymbol{t} \times \boldsymbol{n}$. It is recalled that the curvature κ and divergence $\theta = \operatorname{div} \boldsymbol{t}$ of the fibre lines are given by (15.1,2). In the case of the fluid velocity $\boldsymbol{q}$, the expression

$$\omega^q = -\frac{v_n}{\psi} + \frac{w_s}{\rho_s} + \kappa v + \theta w \tag{38}$$

may be evaluated on use of the relations (10), (11), and (12). Remarkably, a straightforward but somewhat lengthy calculation reveals that the terms involving x_τ and y_τ cancel each other and the vorticity admits a compact representation, namely

$$\omega^q = 2\varphi_\tau + \frac{\rho_{n\tau}}{\psi} + \frac{\rho_{sn}\rho_\tau}{\rho_s \psi} = \left(\partial_\tau - \frac{\rho_\tau}{\rho_s}\partial_s\right)\left(2\varphi + \frac{\rho_n}{\psi}\right). \tag{39}$$

On the other hand, it may also be shown that, as in the steady case [25],

$$\omega^H = -\frac{1}{\rho_s \psi}\left(\rho_s \rho_n \frac{B}{\psi}\right)_n - \frac{(B\psi)_\rho}{\psi}. \tag{40}$$

In summary, the motions considered here are governed by common solutions $(\rho, \psi(\rho, n), B(\rho))$ of the third-order equation (8) together with the compatible pair (10) and the compatibility condition (36) with ω^q and ω^H given by (39) and (40), respectively.

4 A canonical class of hybrid motions

4.1 Lagrangian coordinates

The transformation laws (20) show that, in terms of the Lagrangian coordinates $(\mathsf{s}, \mathsf{n}, \mathsf{t})$, the compatibility condition (36) admits the conservative form

$$(\psi \omega^q)_\mathsf{t} + (B\omega^H)_\mathsf{n} = 0. \tag{41}$$

In fact, by virtue of (39), we obtain

$$(2\psi\varphi + R)_{\mathsf{tt}} + (B\omega^H)_\mathsf{n} = 0. \tag{42}$$

Here, it is emphasised that ω^H may be expressed entirely in terms of the new (in)dependent variables since

$$\omega^H = -R_\mathsf{s} R \frac{B}{\psi^2} - \frac{1}{\psi}(\partial_\mathsf{n} + R\partial_\mathsf{s})\left(R\frac{B}{\psi}\right) - \frac{(B\psi)_\mathsf{s}}{\psi} \tag{43}$$

does not depend on the quantity ρ_s. Accordingly, if

$$R = R(\mathsf{s}, \mathsf{t}), \quad \psi = \psi(\mathsf{s}), \tag{44}$$

then the magnetic flux $A(\mathsf{s})$ is unconstrained, and the compatibility condition (42) reduces to

$$2\psi\varphi_{\mathsf{tt}} + R_{\mathsf{tt}} = 0. \tag{45}$$

Furthermore, since the second-order equation (25) is a consequence of the pair (24), all solutions of the form (44) of the hybrid fibre-reinforced fluid–magnetohydrodynamic system considered here are encapsulated in the overdetermined system

$$\varphi_\mathsf{s} = -\frac{R_\mathsf{s}}{\psi}, \quad \varphi_\mathsf{n} = \psi_\mathsf{s} + \frac{R R_\mathsf{s}}{\psi}, \quad \varphi_{\mathsf{tt}} = -\frac{R_{\mathsf{tt}}}{2\psi}. \tag{46.1-3}$$

Prior to an analysis of the solutions of the above system, it is enlightening to derive some general properties of the motions encoded in the ansatz (44).

4.2 Geometric and algebraic properties

Integration of (26) leads to a relation of the form

$$F(\rho(s,n,\tau),\tau) = n + \tilde{s}(s,\tau) \tag{47}$$

where $\tilde{s}$ is a function of integration. The non-uniqueness of the coordinate s may then be exploited to set $\tilde{s} = s$ without loss of generality so that, locally,

$$\rho = \rho(z,\tau), \quad z = s + n. \tag{48}$$

In this case, the third-order equation (8) may be integrated once to obtain the nonlinear oscillator equation

$$\rho_{zz} + \psi(\rho)\psi'(\rho) = \mu(\tau)\psi(\rho) \tag{49}$$

which, in turn, admits the first integral

$$\frac{1}{2}\rho_z^2 + \frac{1}{2}\psi^2(\rho) = \Psi(\rho,\tau), \quad \Psi(\rho,\tau) = \mu(\tau)\int^{\rho}\psi(\sigma)\,d\sigma + \nu(\tau). \tag{50}$$

Here, the variable τ enters parametrically.

Remarkably, as pointed out in the steady case [19], the four equations (12) for the Eulerian coordinates x and y may be integrated explicitly to obtain

$$\boldsymbol{r} = \frac{1}{\mu}(\psi\boldsymbol{t} + \rho_z\boldsymbol{n}) \tag{51}$$

for $\mu \neq 0$, where the additive function of integration depending on τ has been neglected. It may be retrieved by applying a standard symmetry of the original (unconstrained) governing equations (1), (2), and (27.1), corresponding to the transition to an, in general, non-inertial frame. Hence, we conclude that the fibre-distribution is rotationally symmetric since

$$\boldsymbol{r}^2 = f_1(z,\tau), \quad \boldsymbol{r}\cdot\boldsymbol{t} = f_2(z,\tau). \tag{52}$$

However, in contrast to the steady case [19], in general, this does *not* apply to the fluid flow so that the motions considered here are genuinely 2+1-dimensional. Interestingly, the magnetic field is rotationally symmetric with the field lines constituting concentric circles. This may be concluded from the relations

$$\boldsymbol{H}^2 = f_3(z,\tau), \quad \boldsymbol{r}\cdot\boldsymbol{H} = 0. \tag{53}$$

Furthermore, if the right-hand side of

$$\boldsymbol{r}^2 = \frac{4\Psi(\rho(z,\tau),\tau)}{\mu^2(\tau)} \tag{54}$$

is bounded above and/or below at any fixed time $t = \tau$, then the fluid is confined to a region which is bounded by one or two circles centred at the origin. In fact, it is shown in the following Section that the motion takes place within an annulus, the size of which changes as a function of time.

4.3 The solution (φ, R, ψ)

The compatibility conditions associated with the system (46.1-3) produce an overdetermined system for the function $R(\mathsf{s},\mathsf{t})$ and $\psi(\mathsf{s})$. In the case $\psi_{\mathsf{s}} = 0$, one obtains a system for R only, namely

$$R R_{\mathsf{ss}} + R_{\mathsf{s}}^2 = 0, \quad R_{\mathsf{s}} R_{\mathsf{tt}} + 2 R_{\mathsf{t}} R_{\mathsf{st}} = 0, \quad R_{\mathsf{stt}} = 0. \tag{55.1,2}$$

Now, the conditions (55.1,2) and (55.1,2) supplemented by their t- and s-derivative, respectively, allow one to eliminate the quantities R_{ss}, R_{tt} and R_{sst} and derive the necessary condition

$$(2 R R_{\mathsf{st}} - R_{\mathsf{s}} R_{\mathsf{t}})^2 + 3 R_{\mathsf{s}}^2 R_{\mathsf{t}}^2 = 0. \tag{56}$$

Hence, since R is real, we are led to the strong constraint $R_{\mathsf{s}} R_{\mathsf{t}} = 0$, corresponding to 'elementary' flows which we set aside.

In the case $\psi_{\mathsf{s}} \neq 0$, the compatibility of (46.1-3) leads to

$$\Xi_{\mathsf{tt}} = 0, \quad \Xi = \frac{(\psi R)_{\mathsf{s}}}{\psi \psi_{\mathsf{s}}}. \tag{57}$$

The overdetermined system of compatibility conditions for (46.1-3) may be closed in the sense of Riquier–Janet theory [28] by adding all integrability conditions. Specifically, the *rif* algorithm recorded in [29] and implemented in the computer algebra software Maple [30] may be successfully employed to show that the corresponding involutive system includes the constraint $\Xi^2 + 4 = 0$ in the case $R_{\mathsf{tt}} \neq 0$. Accordingly, the existence of real solutions requires that

$$R_{\mathsf{tt}} = 0. \tag{58}$$

Since $R_{\mathsf{n}} = 0$, it is easy to solve the system (46.1-3) subject to (58). Indeed, after the dependence on n and t has been separated according to

$$\varphi = (\alpha \mathsf{t} + \beta)\mathsf{n} + f(\mathsf{s})\mathsf{t} + g(\mathsf{s}), \quad R = h(\mathsf{s})\mathsf{t} + k(\mathsf{s}), \tag{59}$$

one is left with the ordinary differential equations

$$f_{\mathsf{s}} = 0, \quad g_{\mathsf{s}} = -\frac{\alpha}{h}, \quad h_{\mathsf{s}} = 0, \quad k_{\mathsf{s}} = \alpha \frac{\psi}{h}, \quad \psi_{\mathsf{s}} = \beta - \alpha \frac{k}{h}. \tag{60}$$

If we take into account the non-uniqueness in the definition of the variables s, n, and ψ (subject to the preservation of (48)), the arbitrariness of the 'origin' of time t and that, without loss of generality, we may scale x, y, and t and rotate the (x, y)-plane in which the motion takes place, then the corresponding constants of integration in the solution of the system (60) may be neglected, and it may be assumed that $\alpha = 1$ and $\beta = 0$. Hence, we obtain

$$f = 0, \quad g = -\mathsf{s}, \quad h = 1, \quad k = \cos \mathsf{s}, \quad \psi = -\sin \mathsf{s} \tag{61}$$

so that the solution of the system (46.1-3) is given by

$$\varphi = \mathsf{n}\mathsf{t} - \mathsf{s}, \quad R = \mathsf{t} + \cos \mathsf{s}, \quad \psi = -\sin \mathsf{s} \tag{62}$$

as may be directly verified.

Integration of the differential equation (26) results in

$$\rho = 2 \arctan \left[\sqrt{\frac{\tau + 1}{\tau - 1}} \tan \left(\frac{\sqrt{\tau^2 - 1}}{2} \big(z + z_0(\tau) \big) \right) \right]. \tag{63}$$

It is noted that even though this quantity changes its nature for $\tau < 1$ and in the limit $t \to 1$, it remains real. By construction, ρ is a solution of the differential equation (49) with $\mu = \tau$, that is, the 'stationary' double sine-Gordon equation [31]

$$\rho_{zz} + \sin \rho \cos \rho + \tau \sin \rho = 0. \tag{64}$$

It is observed that the above differential equation is invariant under $\tau \to -\tau$, $\rho \to \rho + \pi$ which is consistent with (63) if the function of integration z_0 is taken into account. It is seen below that this invariance is reflected by a time reversal symmetry of the fluid flow.

The curvature (15.1,2) of the fibre lines is given by

$$\kappa = -\frac{\rho_{zz}}{\rho_z \psi} = -\frac{R_{\mathsf{s}}}{\psi} = -1 \tag{65}$$

so that the fibres constitute circles of unit radius. In fact, it is natural to consider the semicircular fibres $\boldsymbol{r}(\mathsf{s}, \mathsf{n}, \mathsf{t})$, $\mathsf{s} \in [0, \pi]$ which foliate the region occupied by the fluid at any time $t = \mathsf{t}$. Indeed, evaluation of (51) delivers

$$x = \sin(\mathsf{s} - \mathsf{nt}) - \frac{\sin(\mathsf{nt})}{\mathsf{t}}, \quad y = \cos(\mathsf{s} - \mathsf{nt}) + \frac{\cos(\mathsf{nt})}{\mathsf{t}} \tag{66}$$

so that

$$x^2 + y^2 = \frac{\mathsf{t}^2 + 2\mathsf{t}\cos\mathsf{s} + 1}{\mathsf{t}^2}. \tag{67}$$

Accordingly, the fluid flow is confined to an annulus, namely the region between two concentric circles of radii

$$\frac{|\mathsf{t} \pm 1|}{|\mathsf{t}|} \tag{68}$$

given by $\boldsymbol{r}(\mathsf{s} = 0, \mathsf{n}, \mathsf{t})$ and $\boldsymbol{r}(\mathsf{s} = \pi, \mathsf{n}, \mathsf{t})$ for any fixed time t. It is evident that these two circles are convected by the fluid as required. As $\mathsf{t} \to \infty$, the two circles approach each other and coalesce into a unit circle centred at the origin.

4.4 The fluid flow

Since the mapping $(x, y) \mapsto (\mathsf{s}, \mathsf{n})$ is multi-valued if n is not restricted, the fluid velocity $\boldsymbol{q} = \boldsymbol{r}_{\mathsf{t}}$ given by

$$\begin{aligned} q^{(x)} &= \frac{-\mathsf{nt}^2\cos(\mathsf{s} - \mathsf{nt}) - \mathsf{nt}\cos(\mathsf{nt}) + \sin(\mathsf{nt})}{\mathsf{t}^2} \\ q^{(y)} &= \frac{\mathsf{nt}^2\sin(\mathsf{s} - \mathsf{nt}) - \mathsf{nt}\sin(\mathsf{nt}) - \cos(\mathsf{nt})}{\mathsf{t}^2} \end{aligned} \tag{69}$$

is multi-valued. In fact, on taking into account that $\mathsf{s} \in [0, \pi]$, inversion of (66) leads to

$$\begin{aligned} \mathsf{s} &= \arccos\left[\frac{\mathsf{t}^2(x^2 + y^2 - 1) - 1}{2\mathsf{t}}\right], \\ \mathsf{nt} &= \arg(x + iy) - \arctan\left[\frac{1 + \mathsf{t}\cos\mathsf{s}}{\mathsf{t}\sin\mathsf{s}}\right] \end{aligned} \tag{70}$$

so that the multiplicity of the coordinate transformation is encoded in the angle $\arg(x + iy)$. If we choose its principal value contained in the interval $(-\pi, \pi]$, then we obtain a vector field $\boldsymbol{q}$ which is single-valued but discontinuous on the negative x-axis. This vector field is displayed in Figure 1 at time $\mathsf{t} = 2$.

The latter reveals the existence of a 'hyperbolic' stagnation point. Indeed, it is readily shown that $\boldsymbol{q} = \boldsymbol{0}$ if and only if

$$s = \pi - \arccos\frac{1}{\mathsf{t}}, \quad \mathsf{n} = \frac{1}{\sqrt{\mathsf{t}^2(\mathsf{t}^2 - 1)}}. \tag{71}$$

Accordingly, a (moving) stagnation point exists if $|\mathsf{t}| \geq 1$ and is located at

$$x = \sqrt{1 - \frac{1}{\mathsf{t}^2}}\cos\left[\frac{\mathsf{t}}{\sqrt{\mathsf{t}^2(\mathsf{t}^2 - 1)}}\right], \quad y = \sqrt{1 - \frac{1}{\mathsf{t}^2}}\sin\left[\frac{\mathsf{t}}{\sqrt{\mathsf{t}^2(\mathsf{t}^2 - 1)}}\right]. \tag{72}$$

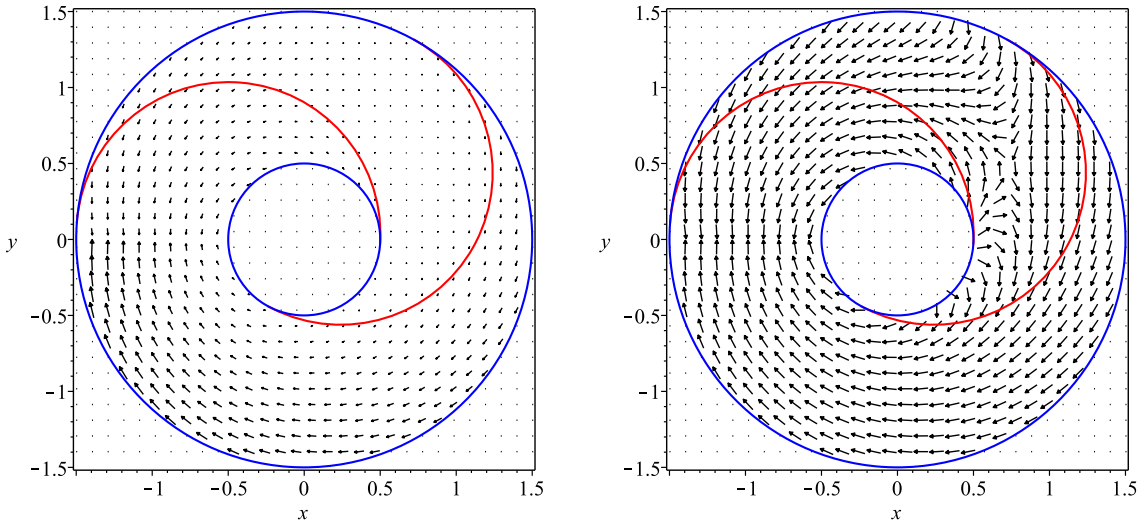

Fig. 1 Left: The fluid velocity $\boldsymbol{q}$ at time $\mathsf{t} = 2$, corresponding to the principal value in the coordinate transformation (70). Right: The normalised vector field, revealing, in particular, the 'hyperbolic' stagnation point. The two red semicircles represent the fibre lines $\mathsf{n} = -\frac{1}{4}$ and $\mathsf{n} = \frac{3}{4}$ which are convected by the fluid

Since the fibre lines are convected by the fluid, it is admissible to restrict the time-dependent region in which the motion takes place to a region which is bounded by two fibre lines corresponding to $\mathsf{n} = \mathsf{n}_{\min}$ and $\mathsf{n} = \mathsf{n}_{\max}$ and the concentric circles enclosing the annulus. For instance, if one chooses $\mathsf{n}_{\min} = -\frac{1}{4}$ and $\mathsf{n}_{\max} = \frac{3}{4}$, then, at the initial time $\mathsf{t} = 2$, the region indicated in Figure 1 is obtained in which the fluid velocity (69) is single-valued. Since this region contains the stagnation point, the fluid particles which are close to the fibre line $\mathsf{n} = \mathsf{n}_{\min}$ move towards the unit circle in a clockwise manner, while the motion of the fluid particles close to the fibre line $\mathsf{n} = \mathsf{n}_{\max}$ is anticlockwise. Figure 2 depicts a sample of the fibre lines at times $\mathsf{t} = 2, 3, 4, 5, 6$.

The blue dotted lines are the curves $\mathsf{s} = \text{const}$. Accordingly, the distance between (the particles on) any such curves along the fibre lines is constant. At time

$$\mathsf{t} = \frac{2\pi}{\mathsf{n}_{\max} - \mathsf{n}_{\min}} = 2\pi, \tag{73}$$

the fibre lines $\mathsf{n} = \mathsf{n}_{\min}$ and $\mathsf{n} = \mathsf{n}_{\max}$ meet, and the fluid particles begin to mix. It is noted that the same phenomenon occurs if the stagnation point is initially not part of the region in which the motion takes place. Eventually, the faster part of the fluid catches up with the slower part, and the particles begin to mix. Figure 3 depicts the fibre line $\mathsf{n} = \frac{3}{4}$ (red) at various times $\mathsf{t} \in [2, 6]$ and the associated particle lines $\mathsf{s} = \text{const}$ (blue).

4.5 A regular solution

As t decreases, the outer radius of the annulus increases and becomes infinite as $\mathsf{t} \to 0$. The inner radius decreases until it vanishes at $\mathsf{t} = 1$, at which point the region in which the motion takes place becomes a disk. If t is reduced further, then the inner radius increases again and becomes infinite as $\mathsf{t} \to 0$. At $\mathsf{t} = 0$, the fluid velocity also becomes singular. In order to obtain a better understanding of the properties of the flow as $\mathsf{t} \to 0$, it is convenient to introduce a non-vanishing function of integration in (51), corresponding to the transition to a non-inertial frame, which ensures that the annulus in which the motion takes place does not move to infinity as $\mathsf{t} \to 0$. As a consequence, the centre of the annulus becomes time dependent and approaches infinity. Similarly, at any fixed time, the magnetic field lines remain concentric circles but their centre moves since it coincides with the centre of the annulus as in the original solution. Specifically, we consider the transition $y \to y - \mathsf{t}^{-1}$, $q^{(y)} \to q^{(y)} + \mathsf{t}^{-2}$ so that the solution of the governing equations is now given by

$$x = \sin(\mathsf{s} - \mathsf{nt}) - \frac{\sin(\mathsf{nt})}{\mathsf{t}}, \quad y = \cos(\mathsf{s} - \mathsf{nt}) + \frac{\cos(\mathsf{nt}) - 1}{\mathsf{t}}, \tag{74}$$

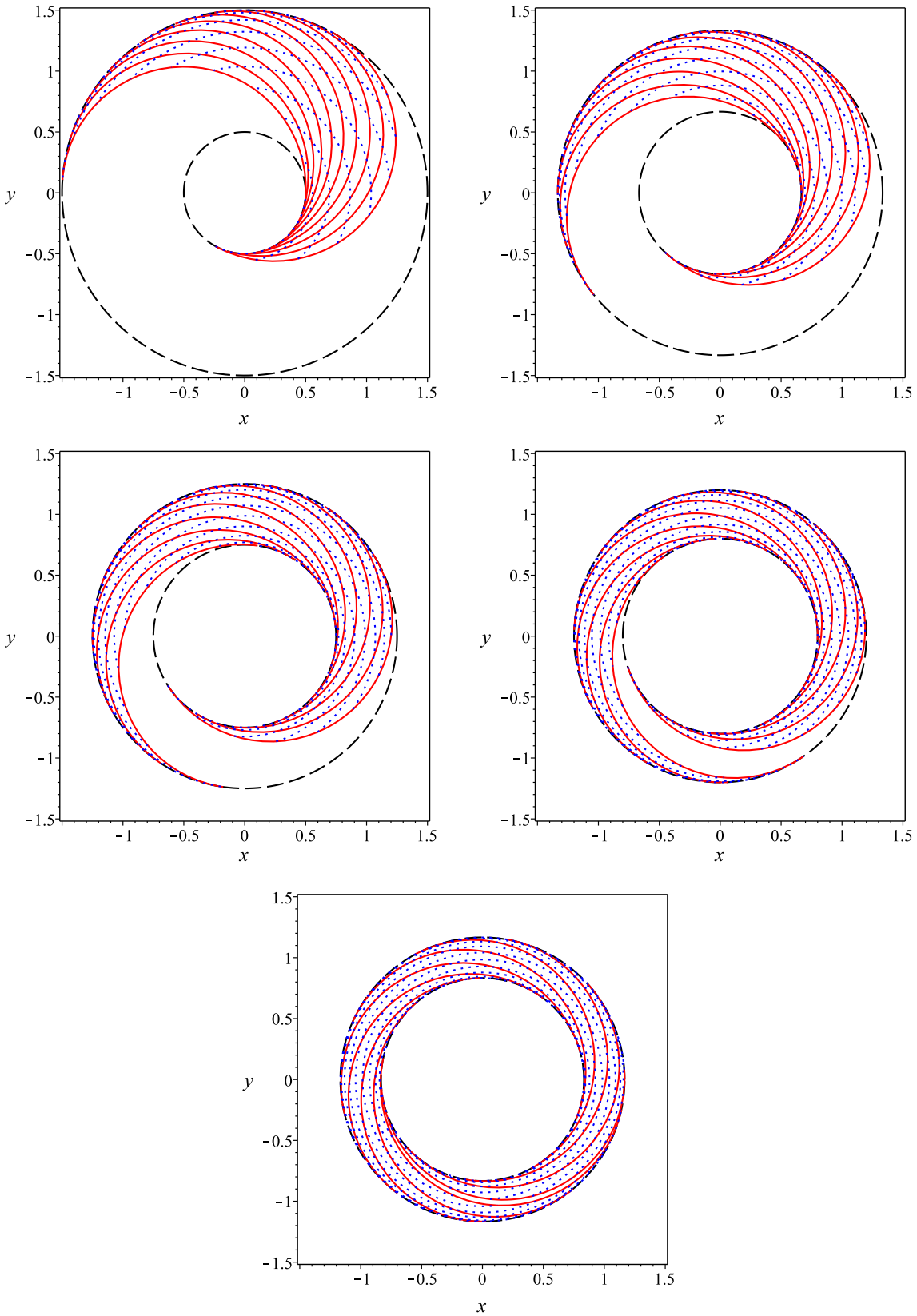

Fig. 2 A sample of the fibre lines $\mathsf{n} \in [-\frac{1}{4}, \frac{3}{4}]$ (red) at times $\mathsf{t} = 2, 3, 4, 5, 6$. The blue dotted lines are the curves $\mathsf{s} = \text{const}$

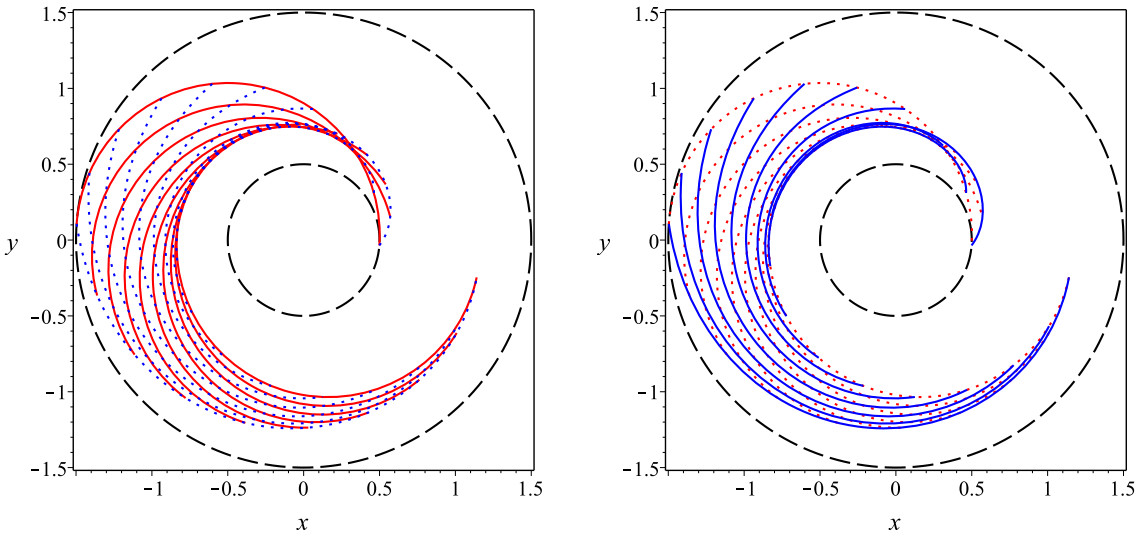

Fig. 3 The fibre line $\mathsf{n} = \frac{3}{4}$ (red) at various times $\mathsf{t} \in [2, 6]$ and the associated particle lines $\mathsf{s} = \text{const}$ (blue)

and

$$q^{(x)} = \frac{-\mathsf{n}\mathsf{t}^2 \cos(\mathsf{s} - \mathsf{n}\mathsf{t}) - \mathsf{n}\mathsf{t}\cos(\mathsf{n}\mathsf{t}) + \sin(\mathsf{n}\mathsf{t})}{\mathsf{t}^2},$$
$$q^{(y)} = \frac{\mathsf{n}\mathsf{t}^2 \sin(\mathsf{s} - \mathsf{n}\mathsf{t}) - \mathsf{n}\mathsf{t}\sin(\mathsf{n}\mathsf{t}) - \cos(\mathsf{n}\mathsf{t}) + 1}{\mathsf{t}^2}, \tag{75}$$

which is regular at $\mathsf{t} = 0$. Indeed, at $\mathsf{t} = 0$, we obtain

$$x = \sin\mathsf{s} - \mathsf{n}, \quad y = \cos\mathsf{s}, \quad q^{(x)} = -\mathsf{n}\cos\mathsf{s}, \quad q^{(y)} = \mathsf{n}\sin\mathsf{s} - \frac{1}{2}\mathsf{n}^2 \tag{76}$$

so that the fluid flow is confined to a horizontal strip bounded by the lines $y = \pm 1$. The multi-valued connection between the Eulerian coordinates x, y and the Lagrangian coordinates s, n is now given by (70) with y replaced by $y + \mathsf{t}^{-1}$, that is,

$$\mathsf{s} = \arccos\left[\frac{\mathsf{t}^2[x^2 + (y + \mathsf{t}^{-1})^2 - 1] - 1}{2\mathsf{t}}\right],$$
$$\mathsf{n}\mathsf{t} = \arg[x + i(y + \mathsf{t}^{-1})] - \arctan\left[\frac{1 + \mathsf{t}\cos\mathsf{s}}{\mathsf{t}\sin\mathsf{s}}\right]. \tag{77}$$

The fluid velocity $\boldsymbol{q}$ at $\mathsf{t} = 0$ is depicted in Figure 4 where, once again, the principal value of arg has been taken.

Figure 4 reveals two features of the fluid flow. On the one hand, there exists a fibre line on which the fluid velocity vanishes. In fact, inspection of the normalised vector field shows that the normalised velocity becomes tangent but changes its direction across this 'stagnation line'. This privileged fibre line is stationary and may be interpreted as a fixed boundary past which the fluid flows. Indeed, it is evident that $\boldsymbol{q} = \boldsymbol{0}$ at $\mathsf{n} = 0$ for all t and $\mathsf{s} \in [0, \pi]$. Figure 5 displays a sample of the fibre lines at times $\mathsf{t} = 0, \frac{1}{2}, 1, \frac{3}{2}, 2, \frac{5}{2}$.

The orange semicircle $x^2 + y^2 = 1$, $x \geq 0$ represents the stationary fibre line $\mathsf{n} = 0$. The motion is chosen to take place in the region bounded by the fibres $\mathsf{n} = \mathsf{n}_{\min} = -1$ and $\mathsf{n} = \mathsf{n}_{\max} = 1$. As time progresses, the strip becomes an annulus of finite radius until it degenerates at $\mathsf{t} = 1$ to a disk of radius 2. The inner radius then starts increasing and the outer radius continuous to decrease. Figure 6 depicts the fibre line $\mathsf{n} = 1$ (red) at various times $\mathsf{t} \in [0, \frac{5}{2}]$ and the associated particle lines $\mathsf{s} = \text{const}$ (blue).

Secondly, Figure 4 indicates that the points on the fibre line $\mathsf{n} = 0$ are not the only stagnation points. In fact, the 'elliptic' stagnation point at $\mathsf{t} = 0$ is located at $(-1, 0)$ since $\boldsymbol{q}(\mathsf{s} = \frac{\pi}{2}, \mathsf{n} = 2) = \boldsymbol{0}$ by virtue of (76).

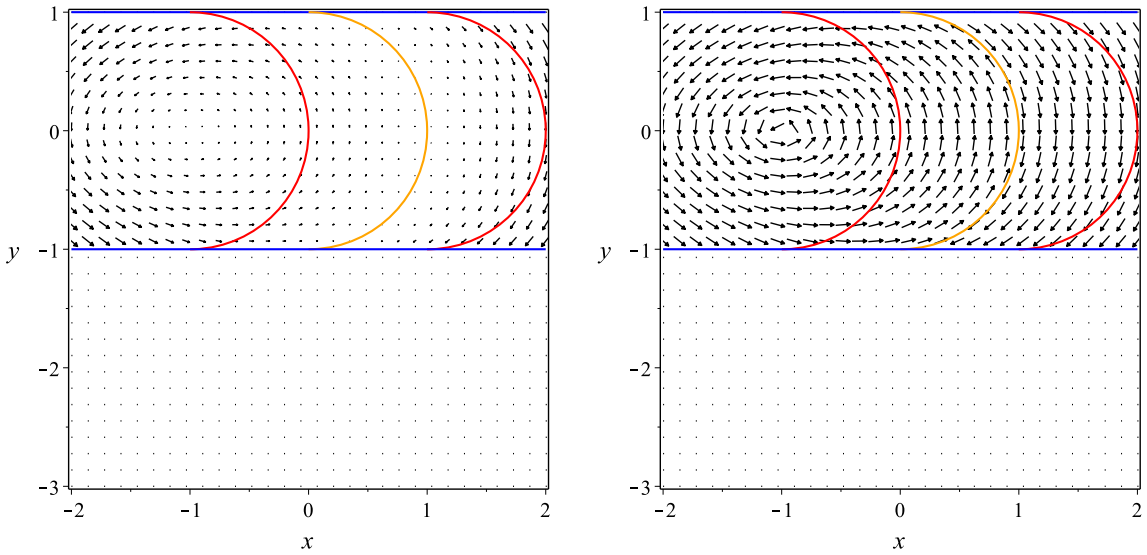

Fig. 4 Left: The fluid velocity $\boldsymbol{q}$ at time $\mathsf{t} = 0$, corresponding to the principal value in the coordinate transformation (77). Right: The normalised vector field, revealing a rotating magnetohydrodynamic motion and, in particular, an 'elliptic' stagnation point. The two red semicircles represent the fibre lines $\mathsf{n} = -1$ and $\mathsf{n} = 1$ which are convected by the fluid. The orange fibre line $\mathsf{n} = 0$ is stationary

In general, excluding $\mathsf{n} = 0$, the condition $\boldsymbol{q} = \boldsymbol{0}$ leads to the pair

$$\sin \mathsf{s} = \frac{1 - \cos(\mathsf{nt})}{\mathsf{nt}^2}, \quad \cos \mathsf{s} = \frac{\sin(\mathsf{nt}) - \mathsf{nt}}{\mathsf{nt}^2}, \tag{78}$$

which immediately implies that we require that $\mathsf{n} > 0$ by virtue of $\mathsf{s} \in [0, \pi]$ and any additional stagnation point is located on the other half of the unit circle $x^2 + y^2 = 1$, $x \leq 0$ since it is readily verified that

$$x = -\sin \mathsf{s}, \quad y = \cos \mathsf{s}. \tag{79}$$

The compatibility condition $\sin^2 \mathsf{s} + \cos^2 \mathsf{s} = 1$ produces the transcendental equation

$$\mathsf{n}^2\mathsf{t}^4 = 2 - 2\mathsf{nt}\sin(\mathsf{nt}) + \mathsf{n}^2\mathsf{t}^2 - 2\cos(\mathsf{nt}). \tag{80}$$

If we focus on non-negative times, then its solution may be parametrised according to

$$\mathsf{t} = \frac{\Delta}{\mathsf{m}}, \quad \mathsf{n} = \frac{\mathsf{m}^2}{\Delta}, \quad \Delta = \sqrt{2 - 2\mathsf{m}\sin \mathsf{m} + \mathsf{m}^2 - 2\cos \mathsf{m}} \tag{81}$$

so that

$$\mathsf{s} = \arccos\left(\frac{\sin \mathsf{m} - \mathsf{m}}{\Delta}\right). \tag{82}$$

In Figure 7, the quantities t, n, and s are plotted against m.

It is observed that, at time $\mathsf{t} = 0$, there exists only one stagnation point (apart from those on the fibre line $\mathsf{n} = 0$). As t increases, only one stagnation point remains present until t reaches a certain value t_2 at which another stagnation point appears. The latter subsequently splits into two stagnation points. As t approaches 1, more and more stagnation points emerge, and there exists an infinite number of coalescing stagnation points at $\mathsf{t} = 1$ located at $(0, -1)$ where all fibre lines meet. As t increases further, the number of stagnation points becomes finite again and decreases until only one stagnation point is left at some time $\mathsf{t} = \mathsf{t}_{\max}$. At any later time, no stagnation points exist.

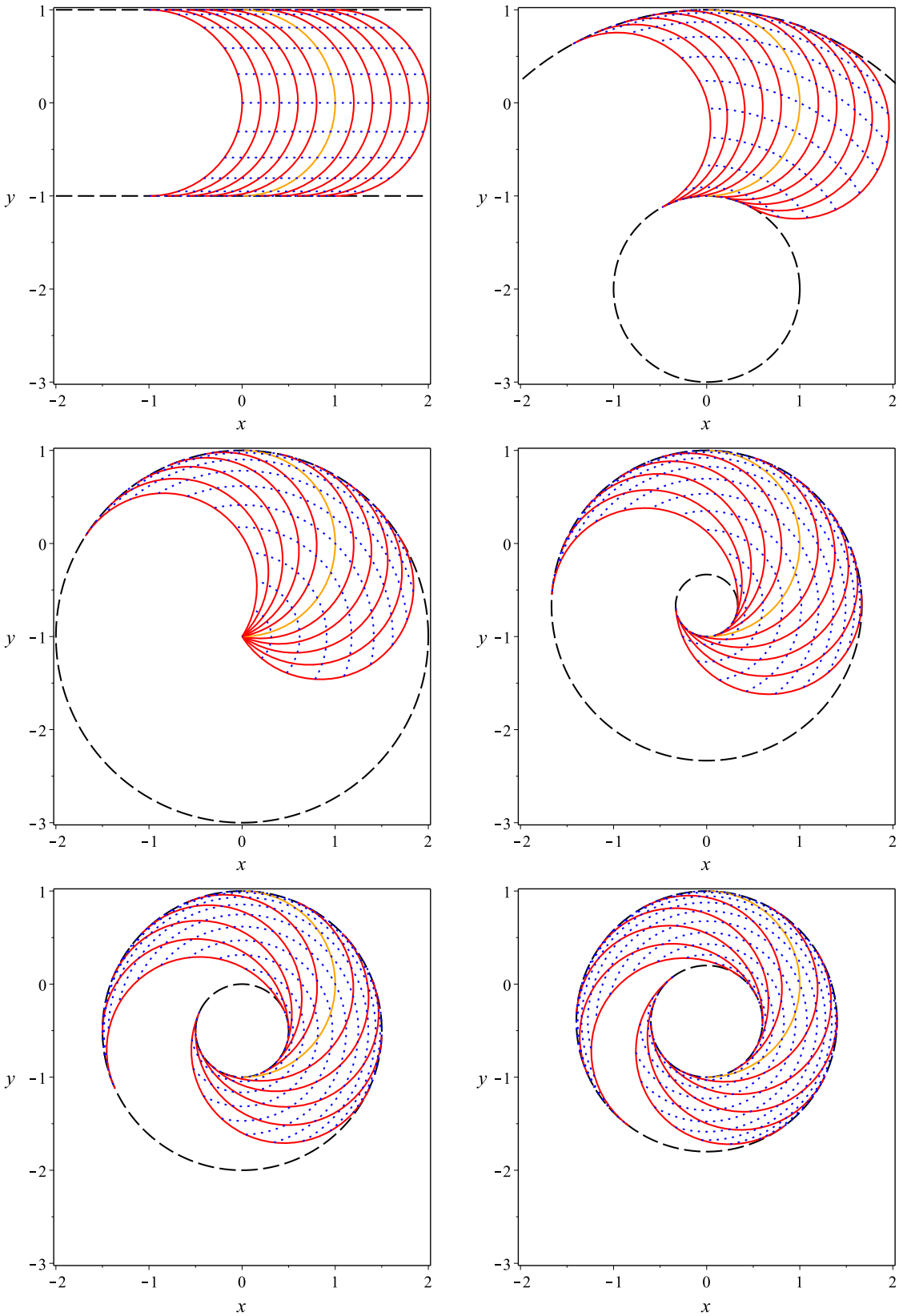

Fig. 5 A sample of the fibre lines $\mathsf{n} \in [-1, 1]$ (red) at times $\mathsf{t} = 0, \frac{1}{2}, 1, \frac{3}{2}, 2, \frac{5}{2}$. The orange fibre line $\mathsf{n} = 0$ is stationary

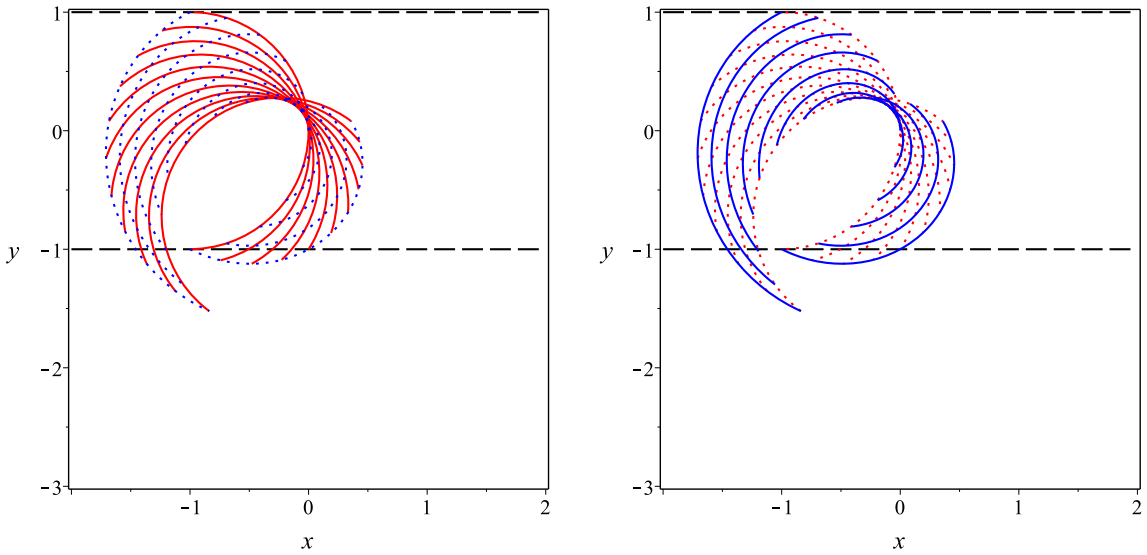

Fig. 6 The fibre line $\mathsf{n} = 1$ (red) at various times $\mathsf{t} \in [0, \frac{5}{2}]$ and the associated particle lines $\mathsf{s} = \text{const}$ (blue).

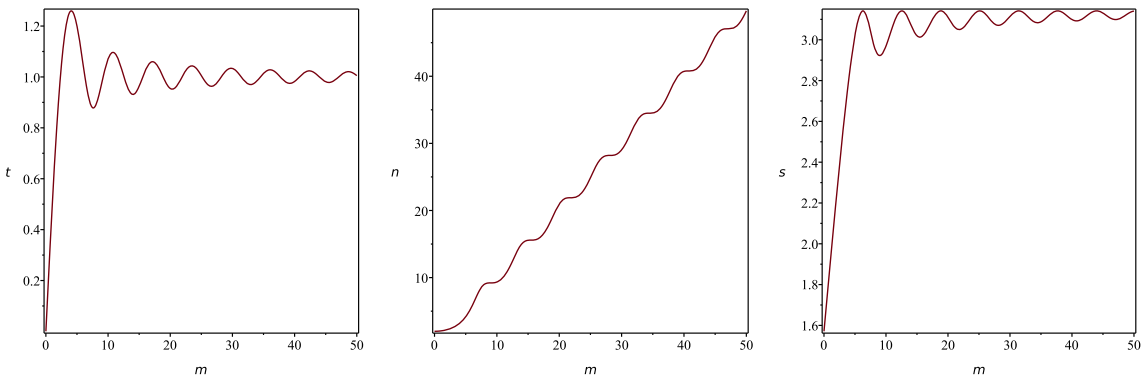

Fig. 7 The values of $\mathsf{t}, \mathsf{n}, \mathsf{s}$ corresponding to additional stagnation points parametrised by m which do not lie on the fibre line $\mathsf{n} = 0$

Funding Open Access funding enabled and organized by CAUL and its Member Institutions

References

1. Marris, A.W., Passman, S.L.: Vector fields and flows on developable surfaces. Arch. Rat. Mech. Anal. **32**, 29–86 (1969)
2. Rogers, C., Kingston, J.G.: Non-dissipative magnetohydrodynamic flows with magnetic and velocity lines orthogonal geodesics on a normal congruence. SIAM J. Appl. Math. **26**, 183–195 (1974)
3. Rogers, C., Schief, W.K.: Intrinsic geometry of the NLS equation and its auto Bäcklund transformation. Stud. Appl. Math. **101**, 267–287 (1998)
4. Rogers, C., Schief, W.K.: Bäcklund and Darboux Transformations: Geometry and Modern Applications in Soliton Theory, Cambridge Texts in Applied Mathematics, Cambridge University Press (2002)
5. Rogers, C.: On the Heisenberg spin equation in hydrodynamics, Informes de Matématica, Série B 127. Instituto de Matématica Pura e Aplicada, Rio de Janeiro, Brazil (2000)
6. Rogers, C., Schief, W.K.: On geodesic hydrodynamic motions. Heisenberg spin connections. J. Math. Anal. Appl. **251**, 855–870 (2000)

7. Schief, W.K., Rogers, C.: The Da Rios system under a geometric constraint. The Gilbarg problem. J. Geom. Phys. **54**, 286–300 (2005)
8. Gilbarg, D.: On the flow patterns common to certain classes of plane fluid motions. J. Math. Phys. **26**, 137–142 (1947)
9. Rogers, C., Ruggeri, T., Schief, W.K.: On relativistic gasdynamics: invariance under a class of reciprocal transformations and integrable Heisenberg spin connections. Proc. R. Soc. A **476**, 20200487 (2020)
10. Rogers, C., Schief, W.K., Hui, W.H.: On complex-lamellar motion of a Prim gas. J. Math. Anal. Appl. **266**, 55–69 (2002)
11. Rogers, C., Szereszewski, A.: On the geometry of complex-lamellar magneto-hydrodynamics: universal motions. Stud. Appl. Math. **128**, 225–251 (2012)
12. Schief, W.K.: Nested toroidal flux surfaces in magnetohydrostatics. Generation via soliton theory. J. Plasma Phys. **69**, 465–484 (2003)
13. Da Rios, L.S.: Sul moto d'un liquido indefinito con un filetto vorticoso di forma qualunque. Rend. Circ. Mat. Palermo **22**, 117–135 (1906)
14. Levi-Civita, T.: Attrazione Newtoniana dei tubi sottili e vortici filiformi. Annali R. Scuola Norm. Sup. Pisa **1**(1–33), 229–250 (1932)
15. Hasimoto, H.: A soliton on a vortex filament. J. Fluid Mech. **51**, 477–485 (1972)
16. Betchov, R.: On the curvature and torsion of an isolated vortex filament. J. Fluid Mech. **22**, 471–479 (1965)
17. Spencer, A.J.M.: Fibre-streamline flows of fibre-reinforced viscous fluids. European J. Appl. Math. **8**, 209–215 (1997)
18. Schief, W.K., Rogers, C., Murugesh, S.: On the kinematics of 2+1-dimensional motions of a fibre-reinforced fluid. Integrable connections. Quart. J. Mech. Appl. Math. **60**, 49–64 (2007)
19. Schief, W.K., Rogers, C.: The kinematics of fibre-reinforced fluids. An integrable reduction. Quart. J. Mech. Appl. Math. **56**, 493–512 (2003)
20. Rogers, C., Schief, W.K.: The kinematics of the planar motion of ideal fiber-reinforced fluids: an integrable reduction and Bäcklund transformation. Theor. Math. Phys. **137**, 1598–1608 (2003)
21. Bour, E.: Théorie de la déformation des surfaces. J. l'École Polytech **42**, 1–151 (1867)
22. Rogers, C., Shadwick, W.F.: Bäcklund transformations and their applications, Academic Press, Mathematics in Science and Engineering Series, New York (1982)
23. Demskoi, D.K., Schief, W.K.: On non-steady planar motions of fibre-reinforced fluids. Geometry and integrable structure. J. Phys. A Math. Theor. **53**, 494001 (2020)
24. Demskoi, D.K., Schief, W.K.: On steady motions of an ideal fibre-reinforced fluid in a curved stratum. Geometry and integrability. J. Phys. A: Math. Theor. **54**, 505205 (2021)
25. Rogers, C., Schief, W.K.: A two-dimensional magnetohydrodynamic system: geometric decomposition and canonical reduction, to be published in Meccanica (2022)
26. Rogers, C., Schief, W.K.: Novel integrable reductions in nonlinear continuum mechanics via geometric constraints. J. Math. Phys. **44**, 3341–3369 (2003)
27. Eisenhart, L.P.: A treatise on the differential geometry of curves and surfaces. Dover, New York (1960)
28. Seiler, W.: Involution. The Formal Theory of Differential Equations and its Applications in Computer Algebra, Algorithms and Computation in Mathematics Series **24**, Springer, Berlin, Heidelberg (2010)
29. Reid, G.J., Wittkopf, A.D., Boulton, A.: Reduction of systems of nonlinear partial differential equations to simplified involutive forms. Euro. J. Appl. Math. **7**, 635–666 (1996)
30. https://www.maplesoft.com/products/Maple/+
31. Bullough, R.K., Caudrey, P.J.: The double-sine-Gordon equation: wobbling solitons? Rocky Mountain J. Math. **8**, 53–82 (1978)